Contents lists available at ScienceDirect

Journal of Building Engineering

journal homepage: http://ees.elsevier.com

Dust filter of secondary aluminium industry as raw material of geopolymer foams

D. Eliche-Quesada [a,b,*], S. Ruiz-Molina [a], L. Pérez-Villarejo [a], E. Castro [a,b], P.J. Sánchez-Soto [c]

[a] Department of Chemical, Environmental and Materials Engineering, University of Jaén, Campus Las Lagunillas s/n, 23071, Jaén, Spain
[b] Center for Advanced Studies in Earth Sciences, Energy and Environment (CEACTEMA), Universidad de Jaén, Campus Las Lagunillas s/n, 23071, Jaén, Spain
[c] Materials Science Institute of Sevilla (ICMS), Joint Center Spanish National Research Council (CSIC)-University of Sevilla, c/Américo Vespucio 49, 41092, Sevilla, Spain

ARTICLE INFO

Keywords
Geopolymer foams
Alkali-activation
Rice husk ash
Aluminum industry waste
Foaming agent

ABSTRACT

In this work, the use of waste dust filter of secondary aluminum industry (DFA) to obtain geopolymer foams has been studied. The waste was used as source of alumina and foaming agent. As precursor and principal reactive silica supplier rice husk ash was used. Precursors were chemically activated by means of a sodium hydroxide aqueous solution and a commercial sodium silicate solution. The influence of the DFA content or Si/Al molar ratio (4–7) were determined by keeping the Si/Na molar ratio of 0.7 M constant and the concentration of sodium hydroxide in the activating solution equal to 8.5 M. The geopolymer foams obtained were studied by X-ray Diffraction (XRD), adsorption/desorption of nitrogen, infrared spectroscopy (FTIR), and scanning electron microscope (SEM) techniques. The results indicated that geopolymer foams presented low values of bulk density (643–737 kg/m^3) high values of apparent porosity (62–70%), low, but sufficient values of compressive strength (0.5–1.7 MPa) and good values of thermal conductivity (0.131–0.157 W/mK). Lower values of thermal conductivity were obtained for Si/Al = 4 and 5 M ratios, due to the highest apparent porosity and the highest total pore volume. These geopolymer foam materials have similar properties to other construction materials sector such as gypsum boards, foamed concrete, or insulating materials. In addition, its use in other applications of interest such as catalyst support or gas filtration materials could be investigated.

1. Introduction

A large amount of industrial wastes is produced annually in the world. In 2014, Spanish industry generated 38.7 million waste, of which 96.6 wt % were non-hazardous [1]. A large amount of industrial wastes is deposited in landfills, generating serious environmental problems. In recent years, the utilization of biomass to generate electricity and heath has resulted in a significant increase, in order to recover waste and reduce CO_2 emissions into the atmosphere.

In the European Union, becoming the fastest growing renewable energy. Biomass represents more than 5% of the total energy consumed in Spain [2]. At the European level, the General Directorate of Agriculture of the European Commission for the 2016/17 season foresaw a harvested area of 442,000 ha, with a production of 2.86 million tons of rice husk [3]. The 20 wt% of total rice production gives rise to the rice husk by-product in the rice industry. Due to its physical-chemical constitution, the rice husk is hardly biodegraded, and hence many times the husk is left in bulk as an agroindustrial residue. One of the ways to eliminate this waste is by combustion, generating between 18 wt % to 20 wt % of ash based on the weight of rice husk [4]. Rice husk ash (RHA) contains more than 90 wt % silica, which makes it an important source of silica, with small amounts of inorganic salts. Its applications are diverse: manufacture of catalysts, zeolites, graphene, storage/energy condenser, carbon capture, manufacture of silicon chips and silica gels, in the production of silica and activated carbon and in the synthesis of lightweight building insulation materials and geopolymers [5–7].

Aluminum can be almost completely recycled. Due to this fact, there are industrial processes for obtaining secondary or second fusion aluminum, obtained from the transformation of aluminum and scrap, which recycle primary aluminum, giving rise to several by-products. The waste generated in the secondary aluminum melting stage is salt slag (more than 500 kg/MT Al), aluminum slag (less than 10,000 MT/year) and furnace filter fines (more than 35 kg/MT Al [8]. In this study, fines of oven filter, generated in the filters installed in the different emitting sources, such as rotary kilns and chip dryers, are used as the source of aluminum. Currently, a part of this waste is purified and used in the steel industry, or is used as a road cracking sealant, although the majority is, in general, landfilled or disposed without treatment, which is why it causes a severe environmental damage.

The so-called Circular Economy is emerging as an environmental and economic concept whose objective is that the value of materials, resources and products (water, energy, …) continue in the economy for the longest time and the generation of waste is minimal. The aim is

* Corresponding author. Department of Chemical, Environmental and Materials Engineering, University of Jaén, Campus Las Lagunillas s/n, 23071, Jaén, Spain.
E-mail address: deliche@ujaen.es (D. Eliche-Quesada)

https://doi.org/10.1016/j.jobe.2020.101656
Received 28 April 2020; Received in revised form 30 June 2020; Accepted 6 July 2020
Available online xxx
2352-7102/

to implement a new economy, to circulate against the current linear system of our economy (extraction, manufacture, use and disposal). Therefore, the effective use of resources in Europe is one of the most important initiatives of the Europe 2020 strategy in order to generate sustainable, smart and inclusive growth. Currently, this is Europe's main future strategy to generate economic expansion and employment. This strategy supports the shift towards an efficient economy in the use of resources and low carbon emissions, as set out in the EU circular economy measures package presented on 02.12.2015 [9]. Therefore, from a technical, environmental and economic perspective, improving the recovery of waste can mean fewer impacts on the environment, as well as opening new markets and promoting less dependence on imports of raw materials. In addition, there is a need to develop new technological tools to stop the environmental footprint derived from the construction materials manufacturing, by the use of waste or by-products in its formulation.

The cement industry has developed alternative cements, such as cements with additions with which the partial substitution of the Portland cement has been achieved by the incorporation of chemically active additions, such as pozzolans and industrial secondary products such as ash and steel slag [10–13] and the cements of alkaline activation or geopolymer cements, being the most promising green cements, due to their low environmental impact [14,15]. Geopolymers are non-Portland cements obtained from the alkaline activation of different sources of aluminosilicates such as natural minerals, by-products or industrial wastes [16,17].

The geopolymers are considered the materials of the future due to their low environmental impact and high performance relative to the consumption of raw materials, their low consumption of energy, as well as causing a significant reduction, approximately 85%, of CO_2 emissions [18]. Consequently, the production of these new substitute sustainable materials of the traditional ones that generate a lower environmental impact is one of the main strategies to fight against climate change that can contribute very effectively to a future green "revolution" in the sector of non-metallic inorganic building materials.

Chemically, geopolymers or alkali-activated materials are obtained by reaction of silicate and aluminate rich raw materials at temperatures lower than 100 °C [19,20]. Geopolymer foams have high thermal efficiency and environmental benefits are an alternative to materials with low thermal conductivity [21–23]. The production of geopolymers with porous structure requires adding blowing agents as aluminum, zinc or silicon metal powders and hydrogen peroxide [24–29]. In geopolymer foams the geopolymerization reaction and chemical foaming reaction occur simultaneously. Recently, wastes as coconut ash [30], bottom ash from solid waste combustion [31], aluminum potassium slags [32] and paval, a solid waste stream from the aluminum industry [33] have been used as innovative foaming agents. They have been proposed for new applications such as cellular concrete [34], sewage treatment [35], catalyst support [36], gas filtration [37], heavy metal immobilization [38,39] and insulation materials [22].

The novelty of this study is to valorize the hazardous waste, dust filter from the secondary aluminum industry (DFA), used only as a drier in the management of hazardous liquids, sludge and oils, in a new potential application, reducing its accumulation in landfills. The composition of the residue is suitable for use as a raw material for manufacturing geopolymeric foams. The residue is rich in Al_2O_3 and has a high sodium content, which reduces the content of the activating solution to achieve a Na/Si molar ratio of 0.7. At the same time, the waste contains metallic aluminum and aluminum nitride in its composition, therefore, the use of organic raw materials, such as polyurethanes, or hydrogen peroxide, is not required in the process for the formation of porosity, resulting in economic and environmental benefits.

In view of this background, the aim of this study is to investigate the use of a waste, not employed so far, dust filter from the secondary aluminum production industry (DFA) as a source of aluminum and bloating agent in the production of geopolymer foams. Other waste, rice husk ash (RHA) was use as a silica precursor. Both raw materials were alkaline-activated by means of a mix solution of sodium hydroxide and commercial sodium silicate. The influence of DFA content or Si/Al molar ratio has been studied.

2. Materials and methods

2.1. Materials

The geopolymers were prepared using as a source of silica, rice husk ash (RHA) and as a source of aluminum and foaming agent, dust filter of secondary aluminum industry (DFA). RHA come from a rice producing industry located in San Juan de Aznalfarache (Seville, Spain). DFA was obtained from Befesa, a service company specializing in the recycling of steel dust, salt slags and aluminum waste located in Erandio (Vizcaya, Spain). RHA was sieved in order to obtain a particle size less than 150 μm. DFA was used as received. A mixture of aqueous sodium silicate (Panreac, SA) with a composition of 8.9 wt % of Na_2O, 29.2 wt % of SiO_2 and 61.9 wt % of H_2O and a 8.5 M NaOH solution (Panreac SA) was used as an alkaline activating solution.

2.2. Synthesis of geopolymer foams

Alkali activated foams (GF4; GF5; GF6 and GF7) were prepared using 4 M ratios of Si/Al = 4, 5, 6 and 7; Na/Si = 0.7. The synthesis of the materials was carried out in several stages involving: i) NaOH solution and homogenization of sodium silicate (pH = 13.2); ii) appropriate amounts of raw materials, RHA and DFA were mixed for 5 min in a Proeti mixer; iii) adding the activating solution in 2 min and iv) mixing the mixtures for 10 min (Table 1).

The aluminum residue acts as a chemical foaming agent, since it contains impurities of metallic Al (<1 wt %) and aluminum nitride (>1.5 wt %) that generate the release of hydrogen [40,41] and ammonia into the slurry according to the following reactions:

$$2\,Al + 6\,H_2O \rightarrow 2\,Al(OH)_3 + 3H_2 \quad \text{(Eq. 1)}$$

$$2\,Al + 3H_2O \rightarrow Al_2O_3 + 3\,H_2 \quad \text{(Eq.2)}$$

$$2Al + 6H_2O + 2NaOH \rightarrow 2Na[Al(OH)_4] + 3H_2\uparrow \quad \text{(Eq. 3)}$$

$$AlN + 3H_2O \rightarrow NH_3\uparrow + Al(OH)_3 \quad \text{(Eq. 4)}$$

Table 1
Mix proportions of geopolymeric foam materials.

Sample	Molar Ratio Si/Al	Molar Ratio Na/Si	RHA (g)	DFA (g)	Na_2SiO_3 (g)	H_2O (g)	NaOH (g)	S/L ratio
GF4	4	0.70	14.20	13.40	9.83	14.62	1.66	1.2
GF5	5	0.70	14.20	11.90	9.88	14.90	2.39	1.2
GF6	6	0.70	10.42	8.05	15.00	5.40	1.86	1.0
GF7	7	0.70	12.50	7.59	12.15	11.18	2.75	1.0

The release of hydrogen and ammonia in the reaction medium generates abundant bubbles resulting in the geopolymeric foam. The concentration of DFA was 25, 22, 19 y 16 wt % for Si/Al = 4, 5, 6 and 7, respectively.

Subsequently, the geopolymeric precursor was subjected to 60 °C and a high relative humidity, 99%, during a setting time of 24 h to favor the formation of H_2 and NH_3, the foam expansion and the consolidation, using sealed polyethylene molds. The specimens were then demold and kept at ambient conditions up to the 28-days final curing stage. A schematic of the synthesis of geopolymer foams and a photo of the materials obtained can be seen in Fig. 1.

2.3. Material characterization

To characterize the RHA, DFA and geopolymer foams, a high resolution scanning electron microscope (FESEM), Merlin by Carl Zeiss was used. The measurement of particle size distributions of the wastes was performed using a Mastersizer 2000LF of Malvern Instruments laser diffractometer. The characterization of the different compounds formed during the geopolymerization reaction and to identify the functional groups present in the geopolymers was carried out using infrared spectroscopy (ATR-FTIR). A Vertex 70, Bruker equipment equipped with ATR accessory with diamond crystal model Bruker Platinum was used. The spectra were collected at frequencies between 4000 and 400 cm^{-1} with 64 scans with a scanning speed of 5 kHz and a resolution of 2 cm^{-1}. Crystalline phases of RHA, DFD and geopolymer foams were evaluated with X-ray diffractometry Empyrean with a PIXcel-3D detector of PANalytical. The CuKα, 40 kV and 35 mA radiation was used to obtain the X-ray diffraction patterns, in a 2 theta range between 10 and 60°. The chemical composition of the wastes was determined by X-ray fluorescence (XRF) using the Philips Magix Pro PW-2440 equipment.

The degree of reaction was determined by attacking 1 g of ground and sieved geopolymer at 150 μm with a solution of HCl (1:20). The attacked solid was filtered under vacuum, dried in an oven and calcined at 1000 °C for 3 h [42,43]. The geopolymeric gel dissolves in the acid solution, while the insoluble residue remains in the ash fraction that does not react. The degree of reaction was determined by calculating the loss of mass produced in the attack of the acid to the geopolymer, according to the equation:

$$Degree\ reaction\ (\%) = (1 - mass\ of\ calcined\ sample) * 100 \quad \text{(Eq.5)}$$

A Micrometitics ASAP 2020 equipment was used to determine the characteristics of the pores of powdered geopolymeric foams. From the adsorption-desorption isotherms of N_2 at −196.8 °C, the specific surface area, pore volume and pore size distribution were determined. The Brunauer-Emmett-Teller (BET) method at a P/P_0 value between 0.065 and 0.2 was used to determine the specific surface. The BJH

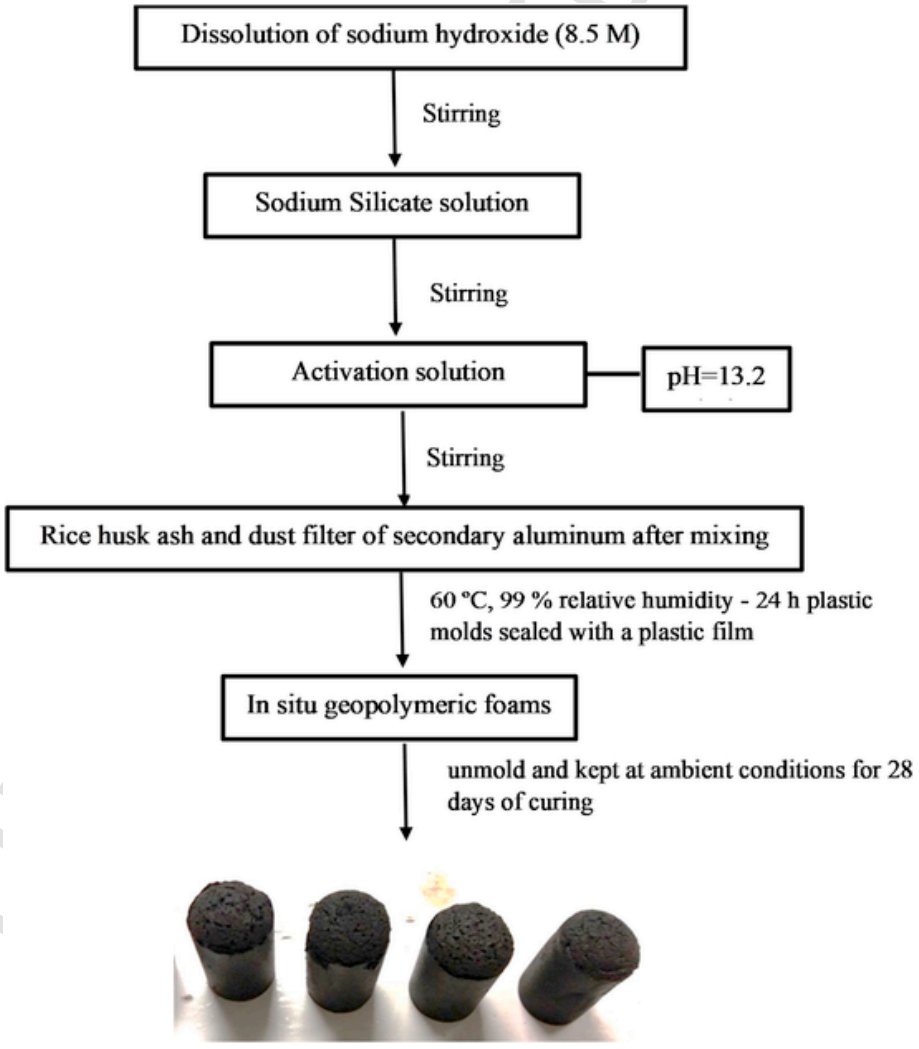

Fig. 1. Synthesis protocol of the geopolymer foams obtained.

method was used to determine the pore volume and pore size distribution. Physical properties such as bulk density and apparent porosity were calculated according to the Archimedes method. European standard UNE-EN 772-21 [44] was followed to determine water absorption. The thermal conductivity of the foamed geopolymers was evaluated by FOX 50 heat flowmeter of TA instrument that utilize a steady state technique for the determination of thermal conductivity, in accordance with ISO 8301 standard [45]. The UNE-EN 772-1 standard [46] was followed to determine the mechanical properties of compressive strength using an MTS 810 Material Testing Systems laboratory press.

3. Results and discussion

3.1. Characterization of raw materials: dust filter of secondary aluminum industry (DFA) and rice husk ash (RHA)

The particle size distribution of the wastes is shown in Fig. 2. The average particle size of the DFA and RHA particles, D_{50}, was 12.5 and 96.2 μm, respectively. The particle size of DFA waste is finer than that of the RHA. The main fraction of the DFA is constituted mainly by particles of the size of the silt (2–63 μm) while RHA consists mainly of sand-sized particles (63–2000 μm) and a minor amount of fine particles (<2000 μm), 1.73 vol % (Table 2).

The specific surface, determined by Blaine permeabilimeter of the DFA was 2058 cm^2/g and of the RHA of 1948 cm^2/g presenting a relative density of 3105 kg/m^3 and 2148 kg/m^3. High specific surfaces have a favorable effect on the chemical reactivity of silica and alumina, since they react at faster speeds when a greater exposed surface is found to be able to react.

XRF was used to determine the chemical composition of the wastes (Table 3). DFA is composed mainly of Al_2O_3 (21.6%) and Na_2O (21.7%) being important its content in Cl- (24.4%) and containing lower amounts in descending order of K_2O, F, S, MgO and CaO. Therefore, DFA can be used as an aluminum and sodium source, raw materials necessary for the formation of geopolymers, besides acting as foamed agent. The main constituents of RHA are SiO_2 (76.7%)

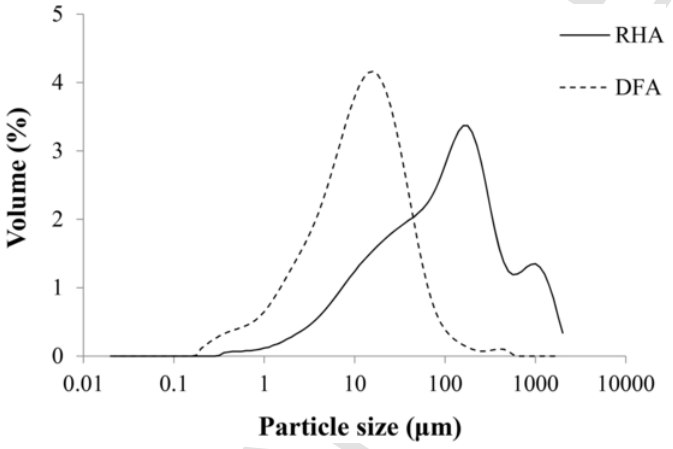

Fig. 2. Particle size distribution of raw materials: dust filter of secondary aluminum industry (DFA) and rice husk ash (RHA).

Table 2
Particle size distribution of raw materials: dust filter of secondary aluminum industry (DFA) and rice husk ash (RHA).

Particle size distribution (mm)	DFA (wt %)	RHA (wt %)
Clay content < 0.002	9.14	1.73
Silt content (0.002–0.063)	84.31	36.86
Sand content (0.063 −2)	6.53	61.41

Table 3
Chemical composition of dust filter of secondary aluminum industry (DFA) and rice husk ash (RHA).

Oxide content (%)	DFA	RHA
SiO_2	0.38	76.7
A_2O_3	21.56	0.183
Fe_2O_3	0.64	0.233
CaO	1.37	0.821
MgO	2.37	0.654
MnO	0.05	–
Na_2O	21.69	–
K_2O	5.88	2.03
TiO_2	0.37	–
P_2O_5	0.03	1.62
SrO		0.035
S	2.69	–
F	2.89	–
Cl	24.42	–
LOI	21.82	17.78

with percentages lower than 3 wt % of other components such as P_2O_5 (1.62%) and K_2O (2.03%). The weight loss by ignition (LOI) is similar although slightly higher in the DFA residue (21.8%) than in the RHA (17.8%). This may be due mainly to the presence of carbonates (18.1% and 5.6%) and organic matter (8.9 and 16.3%), respectively. Both residues have a composition suitable for the formulation of geopolymers [47].

The XRD patterns of the DFA and RHA indicate that both raw materials present crystalline phases. The diffraction pattern of DFA (Fig. 3a) is more complex presenting as main crystalline phases halite (Ref Code: 96-900-6377) NaCl, $K_{3.2}Na_{0.8}Cl_4$ (Ref Code: 96-900-3165), aluminum oxide (Ref Code: 96-152-8428) Al_2O_3, aluminum and magnesium spinel (Ref Code: 96-900-3484) $MgAl_2O_4$, metallic aluminum (Ref Code: 96-901-2430) Al, aluminum nitride (Ref Code: 96-101-0515) AlN, feldspars (silicoaluminate of alkaline and/or alkaline earth, (Ref Code: 96-153-1007) $KAlSi_3O_8$), elpasolite (Ref Code: 96-900-9342) K_2NaAlF_6 and $BaFe_{1.5}Al_{0.5}O_4$ (Ref Code: 96-152-4485). The halite phase could be formed by a process of condensation of gases rich in Na and Cl, when the temperature is lowered to extract the filter dust of the secondary aluminum industry below 801 °C, the melting point of this phase [48]. The main phase of the RHA residue (Fig. 3b) is cristobalite (Ref Code: 96-900-8228) polymorphic form of quartz, formed at high temperatures during the combustion process of rice husk. XRD pattern present a background indicating the present of amorphous phase.

Fig. 4 shows the SEM images of wastes used as raw materials. It is observed that both residues are formed by particles of micrometric size, as well as larger particles, observing a large granulometric distribution. DFA waste reveals the presence of spherical particles, rich in Cl, Na and K, as well as irregular ones, rich in Al according to the FRX and XRD data The RHA particles are formed by silica, the main component of the residue, also containing small amounts of alkaline earth elements according to the EDAX analysis. The particles of the RHA waste are relatively larger.

3.2. Geopolymer foams characterization

Diffraction results from 28-days cured geopolymer foams (Fig. 5) indicate the presence of amorphous substances, when deviations of the baseline were observed between values of 2θ between 20 and 35°. This fact can indicate the formation of an amorphous geopolymer gel produced in the geopolymerization reaction [49,50]. In addition, diffraction peaks are observed, indicating the presence of crystalline structures of SiO_2 (such as cristobalite) (Ref Code: 96-900-8228), NaCl

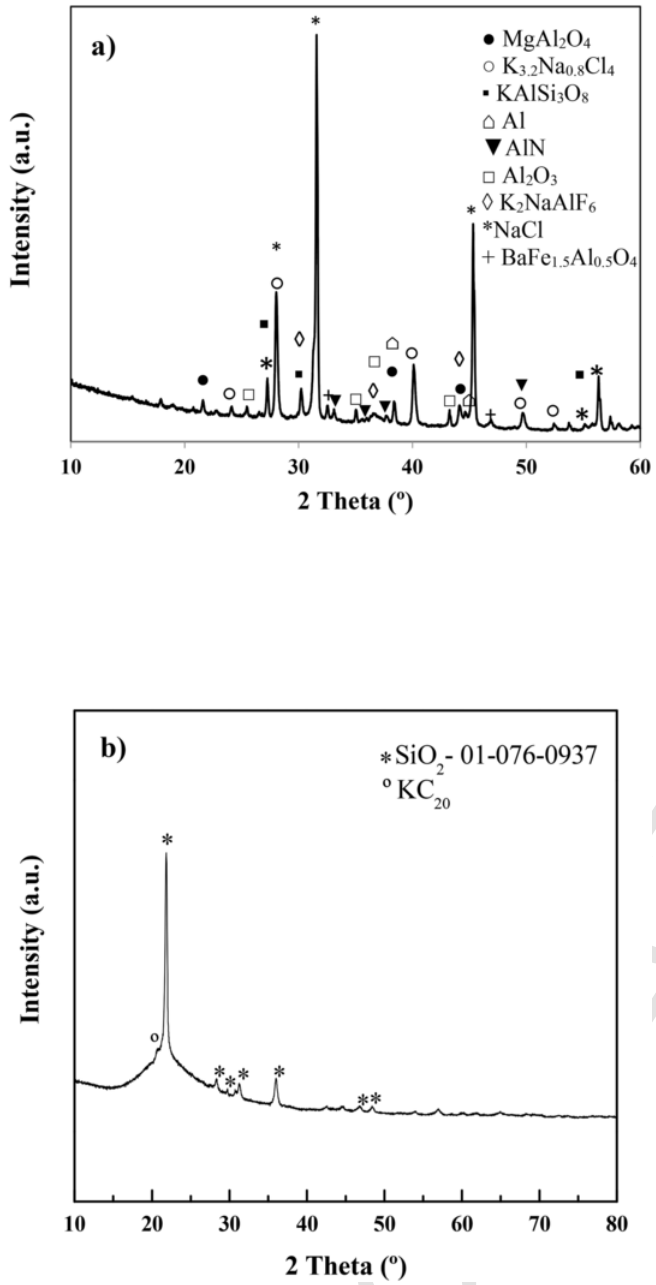

Fig. 3. (a) XRD pattern of dust filter of secondary aluminum industry (DFA) and (b) XRD pattern of rice husk ash (RHA).

(Ref Code: 96-900-6377) and Al_2O_3 (Ref Code: 96-152-8428) in the raw materials. The crystalline phases present in the raw do not intervene in the geopolymerization reaction.

The FTIR analysis was used to know a molecular "fingerprint" of both rice husk ash and geopolymer foams obtained by alkaline activation of the raw materials RHA and DFA (Fig. 6). The dissolution of the waste used as raw material in the alkaline solution is the first stage. A solid network is formed from the polymerization reaction of the species formed by hydrolysis. The dissolution of the aluminates and silicates present in the residues used as raw materials, RHA and DFA, is promoted by the hydroxyl ions present in the alkaline activator that promote an increase in the rate of hydration [51]. The FTIR spectrum allocated at approximately 1100 cm^{-1} is assigned to non-reactive silica-rich particles [52]. The shoulder detected in this spectra region is slightly higher for geopolymer foams with lower Si/Al ratio, which indicates that these samples have a higher number of silica-rich phases, which confirms their lower reaction compared to the formulations with ratios molars Si/Al = 6 and 7. Therefore, for higher molar ratios a higher dissolution of the Si of the RHA raw material is achieved. The bands centered between 1061 and 1011 cm^{-1} correspond to the vibrations stretching asymetric of Si–O–Si in the raw material, RHA waste (1061 cm^{-1}) and Si–O–T (T = Si or Al) bonds of SiO_4 or AlO_4 tetraedra in geopolymer foams (1030-1011 cm^{-1}) [53]. The displacement of the position of the band with respect to the band of the raw material, indicates the activation by the alkaline solution of the raw materials, and therefore, indicates that the geopolymerization reaction takes place [54]. In addition, the displacement indicates that the Al is incorporated into the Si—O—Si structure and there has also been an increase in the number of non-bridging oxygen in the silicon tretrahedra [55]. The peaks centered at 790 cm^{-1} more intense in the raw material RHA could correspond to Si—O stretching characteristic of the bonds that are present in the RHA of origin, mainly in crystalline compounds such as cristobalite. The not very intense peak observed at 617 cm^{-1}, that is only observed in the raw material, could be due to the vibrations of the silanol groups (Si—OH). The band at approximately 440 cm^{-1}, could correspond to the second characteristic band of the sodium aluminosilicate gel characteristic of the deformation vibrations of the T-O-T bonds (T = Al, Si). This band could also be assigned to the angular vibration of deformation of the Si–O–Si bonds present in the raw material RHA. The FTIR analysis confirms that the ash react with the waste of the aluminum industry and become a geopolymer structure.

Figs. 7 and 8 show the nitrogen adsorption/desorption analysis and pore size distribution curves of the geopolymer foams, respectively. All adsorption-desorption isotherms of N_2 conform to type IV with hysteresis cycle, indicating capillary condensation in mesopores according to the IUPAC classification [56]. The H3-type hysteresis cycle is usually due to aggregate flat particles that form slit-like pores [57] as in SEM micrographs it can be observed. The presence of macropores and mesoporos with a non-uniform size is attributed to the vertical asymptotic profile at high relative pressures P/Po that appears in the

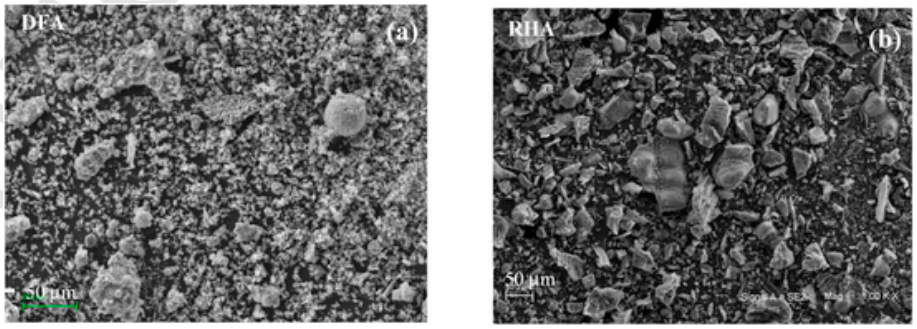

Fig. 4. (a) SEM micrograph of dust filter of secondary aluminum industry (DFA) and (b) SEM micrograph of rice husk ash (RHA).

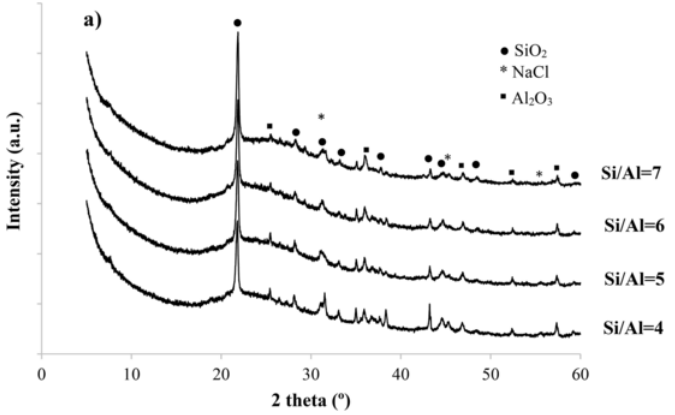

Fig. 5. (a) XRD patter of geopolymer foams as a function of Si/Al molar ratio.

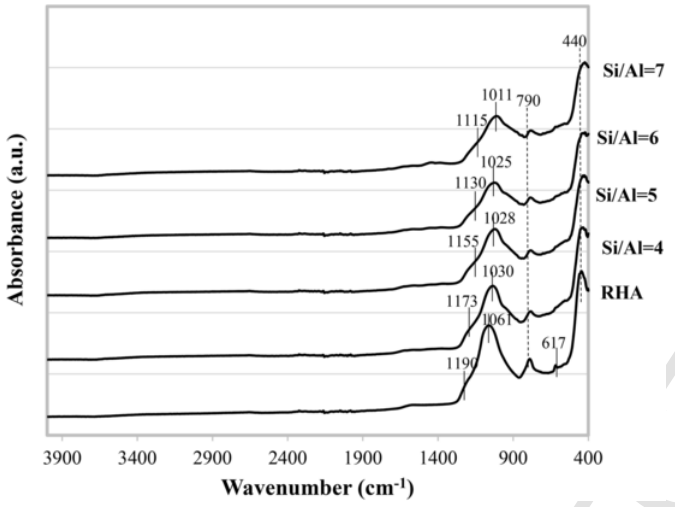

Fig. 6. IR spectra of raw material (RHA) and geopolymer foams as a function of Si/Al molar ratio.

isotherms [58]. All geopolymeric foams have a well -connected pore structure as indicated by the dominant reflections in the mesoporous region (2, 3 and 11 nm) and the presence of macropores (99 nm) [59].

Textural properties of the obtained geopolymer foams are shown in Table 4. The BET specific surface area is greater for the sample Si/Al = 5, showing a beneficial effect of porosity formation for these geopolymer foams. The lower mesoporous area corresponds to the specimens with Si/Al molar ratio of 6. The total pore volumes of geopolymer foams are greater for specimens containing a Si/Al = 5 M ratio indicating a greater connectivity of the pore structure, however geopolymeric foams with a Si/Al = 6 M ratio present a larger pore diameter size (7.36 nm).

The reaction degree is greater with increasing Si/Al molar ratio as shown in Table 5, reaching a maximum value of 61.5% for a Si/Al molar ratio of 7.

The bulk density and apparent porosity data of the geopolymer foams cured for 28 days are show in Table 5. All geopolymeric foams have a low bulk density in the range of 644–709 kg/m^3. The formation of the H_2 and NH_3 bubbles, the increase in viscosity and the consolidation of the foams is favored in the curing stage at 60 °C. The balance of the two mechanisms allows to trap bubbles of H_2 and NH_3, which due to the pressure exerted by the geopolymer paste expand within the structure and give rise to porous foams [60,61]. All foams present an apparent porosity from 62 to 70%. The apparent porosity increases as the bulk density decreases. Among the investigated samples, GF4 exhibits the higher porosity (70.0%) and water absorption (60.9%) and the lowest bulk density (644 kg/m^3). The apparent porosity values are similar to those obtained for geopolymeric foams that use different proportions of rice husk and metakaolin as a precursor and aluminum powder as a foaming agent. The specimens had a porosity between 64.19 and 77.39% depending on the water/metakaolin ratio [62]. However, Dembovska et al. [63], have obtained higher porous geopolymers with higher apparent porosity values between 83 and 86% and lower bulk density between 380 and 470 kg/m^3 using as raw materials metakaolin residue and aluminum scrap recycling waste, metakaolin residue, aluminum scrap recycling waste and glass waste or metakaolin residue, aluminum scrap recycling waste and steel-plant waste.

Images of the core sections of the geopolymeric foams are shown in Fig. 9. Every specimen present a structure with approximately irregular spherical pores derived from the foaming process. The geopolymeric foams with Si/Al = 4 and 5 h M ratios have a brighter surface, while geopolymeric foams with Si/Al = 6 and 7 M ratios present a more spongy structure. In all the foams prolate pores are observed. The structure is more homogeneous in geopolymeric foams with Si/Al = 6 and 7 M ratio, due to the lower solid/liquid ratio in the starting materials (1 for foams with Si/Al = 6 and 7 and 1.2 for foams with Si/Al = 4 y 5).

SEM micrographs (Fig. 10) show the microstructure of the fracture surface of the geopolymeric foams (GF4 and GF7). All specimens show the formation of amorphous porous gel, with closed and interconnected pores of different sizes. All foams are formed by big pores with a large interpores partition where smaller pores are observed.

Thermal conductivity (λ) is an important property in foams as it affects its insulation capacity. The geopolymer foams present values of thermal conductivity between 0.157 W/mK and 0.131 W/mK for geopolymeric foams with Si/Al = 7 and Si/Al = 5 M ratio, respectively (Fig. 11). The Si/Al = 5 samples have a greater total volume of pores generated in the foaming process. The values obtained from thermal conductivity indicate that geopolymeric foams are promising insulating materials. The thermal conductivity values are similar to those obtained for geopolymeric foams using clayed material an iron – aluminum – calcium slag as precursor and 2 wt % potassium – aluminum slag as foaming agent, with thermal conductivity of 0.169 W/mK [64]. Kanseu et al., [62] obtained thermal conductivity values between 0.21 and 0.12 W/mK depending on the water/metakaolin ratio for metakaolin-rice husk ash porous geopolymers that use aluminum powder as a foaming agent.

Normally, the compressive strength of these building materials, light foams, is not a critical factor, since they are not used in loading applications. However, it is important from a transport point of view without damaging its porous structure. The compressive strength data (Fig. 11) indicate that geopolymer foams present low values of this mechanical property due to their high relative porosity. The lowest values of compressive strength, 0.5 MPa, are obtained for specimens with Si/Al = 4 and 5 M ratios. These specimens have a greater total pore volume and greater porosity and lower amount of geopolymeric gel as indicate reaction degree (Table 5). Compressive strength may be determine by the amount of geopolymer gel, the pore size and the pore size distribution. High bulk densities with more homogeneous and lower pores allows a more suitable distribution of the charge within the geopolymer gel. Specimens having a Si/Al = 7 M ratio present the highest compressive strength of 1.7 MPa, because they have a greater bulk density and a smaller total pore volume, smaller size, and a slightly narrower distribution and possibly a greater proportion of geopolymer gel as indicated by the reaction degree. Hajimohammadi et al. [65] obtained geopolymeric foams using fly ash activated as a precursor by alkali solutions which are made from different ratios of alkali activators NaOH and sodium silicate solution and aluminum powder as a foaming agent. The samples presented compressive strenght val-

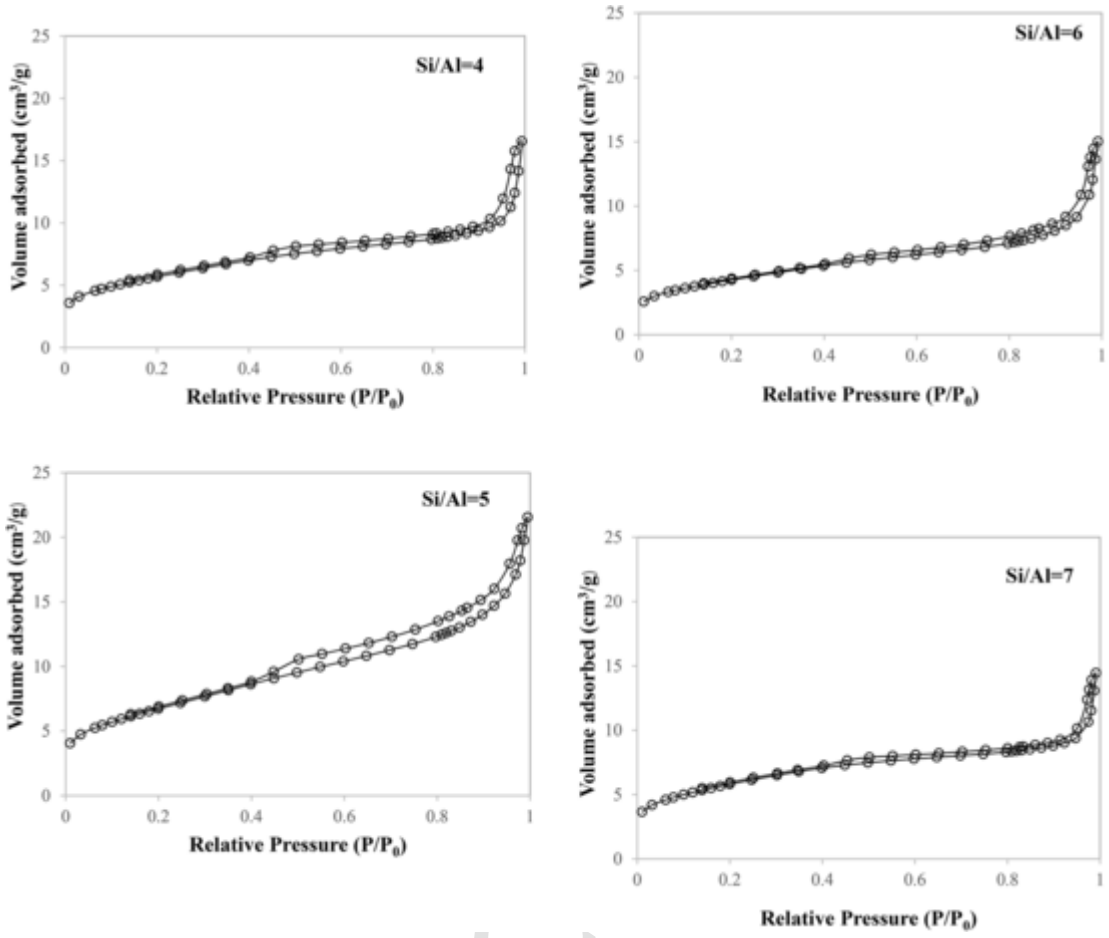

Fig. 7. The nitrogen adsorption/desorption analysis Isotherms of nitrogen adsorption/desorption of geopolymer foams as a function of the Si/Al molar ratio.

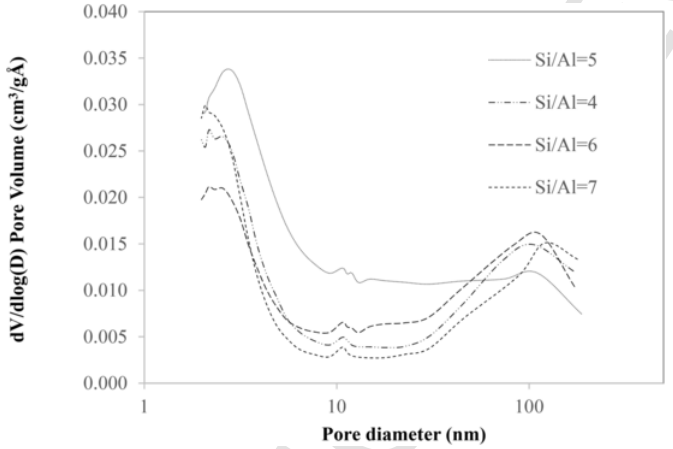

Fig. 8. Pore size distribution curves of the geopolymer foams as a function of the Si/Al molar ratio.

ues between 1.6 and 0.4 MPa, with bulk densities between 880 and 680 kg/m^3, respectively. Dembovska et al. [63] obtained compressive strength values of 1.1 MPa for synthesized geopolymeric foams using waste metakaolin and aluminum scrap recycling waste as raw materials. The incorporation of steel-plant waste produced geopolymers foams with higher compressive strength up to 2.0 MPa. The heat conductivities values ranging between 0.14 and 0.15 W/m·K.

The thermal conductivity and compressive strength of the new geopolymeric foams obtained are similar to other common low thermal conductivity construction materials. Some examples are proposed next: cork board, with thermal conductivity, λ = 0.052–0.70 W/mK and compressive strength of 0.15–2.5 MPa, used for thermal insulation [[70]]; expanded clay with λ = 0.085–0.160 W/mK with sound insula-

Table 4
Textural properties of the foamed geopolymers as function of Si/Al molar ratio determined by nitrogen adsorption/desorption analysis.

Sample	Molar ratio Si/Al	Specific surface área S_{BET} (m^2/g)	Total pore volume $V_{BH,\ ads}$ (cm^3/g)	Average pore diameter $D_{BJH,ads}$ (nm)
GF4	**4**	20.37	0.024	6.58
GF5	**5**	24.32	0.032	6.21
GF6	**6**	15.42	0.022	7.36
GF7	**7**	20.86	0.019	5.79

Table 5
Reaction degree and physical properties of geopolymer foams as function of Si/Al molar ratio.

Molar ratio Si/Al	Reaction degree (%)	Bulk density (kg/m^3)	Apparent porosity (%)	Water absorption (%)
4	48.5	643.94 ± 10.28	69.69 ± 0.37	60.88 ± 2.43
5	53.5	678.95 ± 22.41	63.40 ± 1.76	45.62 ± 3.31
6	54.0	652.48 ± 22.40	65.37 ± 2.06	45.15 ± 5.57
7	61.5	717.82 ± 18.37	62.32 ± 1.22	38.50 ± 3.51

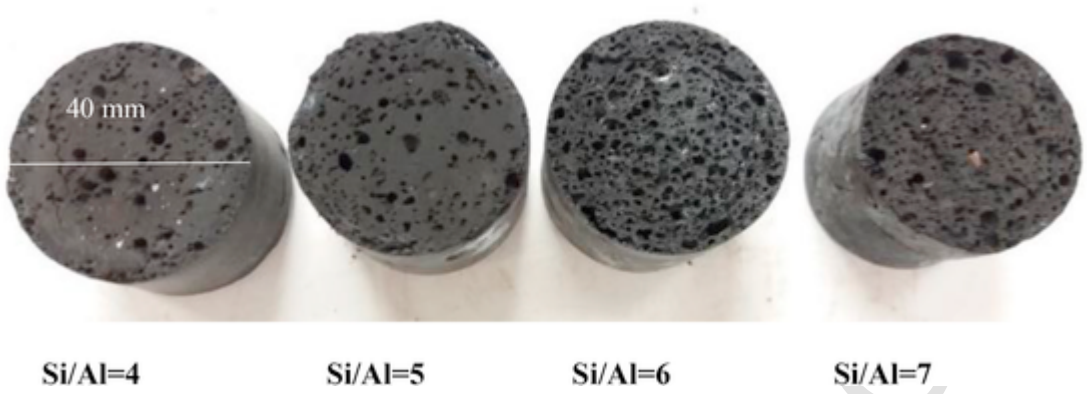

Fig. 9. Photographs of the core sections of the geopolymer foams (cylindrical specimen 40 mm diameter and 50 mm length) as a function of the Si/Al molar ratio.

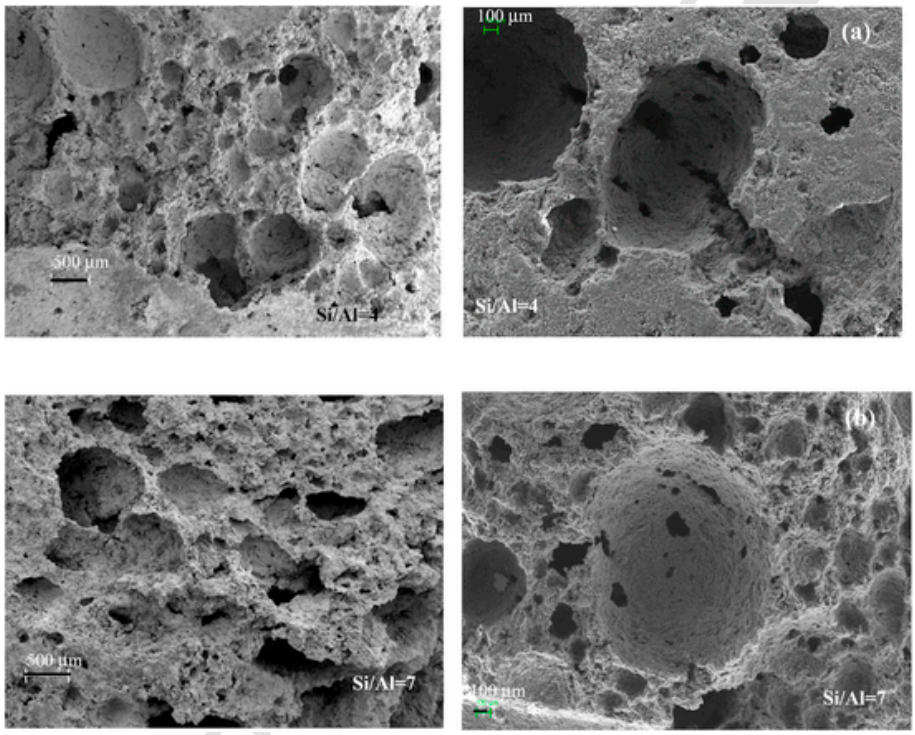

Fig. 10. SEM micrographs of geopolymer foams (a) GP4: Si/Al = 4 M ratio and (b) GP7: Si/Al = 7 M ratio at 40x and 250x.

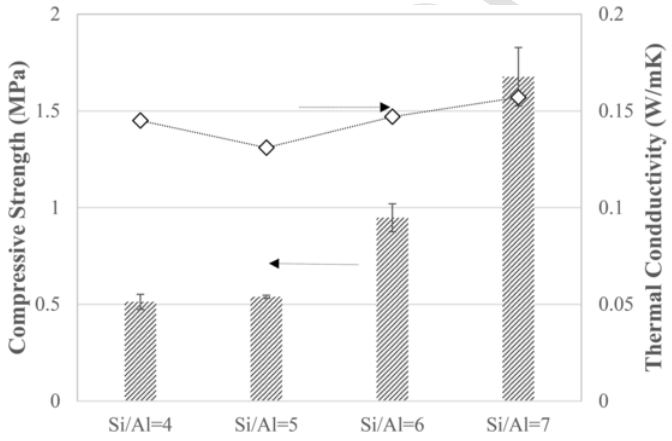

Fig. 11. Compressive strength and thermal conductivity of geopolymer foams as a function of Si/Al molar ratio.

tion applications of suspended floor constructions and aggregate in the manufacture of masonry units [71]; foamed concrete with λ = 0.081–0.19 W/mK and compressive strength ≥ 0.4 MPa with application in exterior protected construction [70] and wood fiber board with λ = 0.11–0.26 W/mK and compressive strength of 0.4–0.5 MPa used in partition board, wall panel and ceiling [70]. In addition, the new geopolymeric foams obtained have lower thermal conductivity and bulk density values than gypsum plasterboard with densities of 900 kg/m^3 and λ = 0.25 W/mK used as partition board and wall panel [72].

3.3. Comparision with other foams geopolymers materials

The physical, mechanical and thermal properties were compared with those of other research. It should be considered that different raw materials, water content, foaming agents and curing regime are used. Ziegler et al. [66] activated fly ash using alkaline solution realized with rice husk ash and KOH, incorporating between 0.05 and 0.3% of aluminum powder as a foaming agent. The porosity of the specimens varies between 54 and 67% with the addition of 0.05 and 0.3% of alu-

minum powder. Geopolymeric foams that incorporate 0.3% aluminum powder have values of apparent porosity and compressive strength similar to those obtained in this study. Palmero et al. [67], used metakaolin and hydrogen peroxide in different amounts as a foamed agent. Geopolymeric foams were obtained with a porosity between 56 and 75%, a bulk density between 590 and 330 kg/m^3, thermal conductivities between 0.15 and 0.17 W/mK, but with higher compressive strengths between 1.8 and 5.2 MPa. Alam Zaidi et al. [68], produced geopolymeric foams using different percentages of natural soil as a source of aluminosilicates and 2 wt % of hydrogen peroxide as a foaming agent. The geopolymeric foams had bulk densities between 1090 and 863 kg/m^3, apparent porosity between 54.0 and 63.1%, compressive strength between 1.6 and 3 MPa and thermal conductivity between 0.267 and 0.334 W/mK. Chen et al. [69], studied the manufacture of geopolymeric foams from bottom ash from the combustion of solid waste that contains a certain amount of metallic aluminum that is used as a foaming agent. Geopolymeric foams with apparent densities between 612 and 1036 kg/m^3, compressive strengths between 0.95 and 2.82 MPa and porosity between 10.3 and 37.3% were obtained. Hassan et al. [30] prepared geopolymer foams using as raw materials coconut ash (CA) and alumina slag (AS). The authors indicated that the incorporation of 7 wt % of AS at coconut ash with a water to CA powder ratio of 0.4 produced geopolymer foams with a bulk density of 640 kg/m^3, a total porosity of 83%, a compressive strength of 1.3 MPa and a thermal conductivity of 0.045 W/mK. Gouloure et al. [73] manufactured geopolymers with insulating properties from metakaolin, volcanic ash and rice ash, using aluminum powders as a foaming agent. The bulk density of geopolymers varies from 600 to 800 kg/m^3. The increase in aluminum powder produced a decrease in thermal conductivity from 0.600 W/mK, typical value of the thermal conductivity of compact metakaolin up to 0.150 W/mK. Font et al. [74] designed geopolymer from fluid cracking catalyst residue (FCC) aerated by recycled aluminium foil powders (R). The geopolymers presented low bulk density (600–700 kg/m^3), relatively high compressive strength (2.5–3.5 MPa), and thermal conductivity between (0.581–0.700 W/mK). Novais et al. [75] manufactured light and porous geopolymers using metakaolin and biomass ash using aluminium as foaming agent. The geopolymers presented bulk density from 850 to 430 kg/m^3, compressive strength of 0.6–4.3 MPa and thermal conductivity of 0.082–0.227 W/mK. All the materials showed similar physical and mechanical properties, however thermal conductivity can differ, finding materials with similar thermal properties, but also with different thermal properties in both directions with major and minor thermal conductivity.

4. Conclusions

Geopolymer foams were prepared using as a source of aluminum and foaming agent, dust filter of secondary aluminum industry, and as source of silica, rice husk ash. The influence of aluminum waste or the Si/Al molar ratio in the formation of foamed geopolymers in the range of 4–7 was investigated. The XRD analysis confirms the formation of the sodium aluminosilicate gel for all the Si/Al molar ratios studied and the 28-day curing time. Nitrogen/desorption analysis demonstrated the mesoporous structure of the geopolymers, being the geopolymeric foams with a Si/Al = 5 M ratio that presents a greater surface area, whereas, geopolymeric foams with a Si/Al = 7 M ratio have the smallest pore diameter. The geopolymer foams have low bulk densities with values between 644 kg/m^3 and 738 kg/m^3, and apparent porosity between 62 y 70%. The mechanical properties, as compressive strength of the geopolymer foams increases with the Si/Al molar ratio, reaching the maximum value of 1.7 MPa for the specimens with a Si/Al = 7 M ratio. The low thermal conductivity values of the geopolymeric foams (0.131 and 0.157 W/mK), confirm their adequate use as insulating materials. The geopolymer foams with Si/Al = 4 and 5 M ratios have greater thermal insulation capacity.

Therefore, sustainable geopolymer foams can be obtained from industrial by-products, by means of processes of low energetic cost, with adequate physical, mechanical and thermal properties for applications of great interest such as support of catalysts, materials for gas filtration, foamed concrete and insulating materials.

Declaration of competing interest

The authors declare that they have no known competing financial interests or personal relationships that could have appeared to influence the work reported in this paper.

Acknowledgement

This work was funded by the Project “Valuation of various types of ash for the obtaining of new sustainable ceramic materials” (UJA2014/06/13), Support Plan of the University of Jaén, sponsored by Caja Rural of Jaén. The authors want to thank “Befesa” and “Herba Ricemills” companies for supplying raw materials for geopolymeric foams production. Technical and human support provided by Scientifical and Technical Instrumental Center (CICT) of Universidad de Jaén (UJA, MINECO, Junta de Andalucía, FEDER) is gratefully acknowledged.

Appendix A. Supplementary data

Supplementary data to this article can be found online at https://doi.org/10.1016/j.jobe.2020.101656.

Uncited reference

[48,69–75].

References

[1] Spanish Statistical Office www.ine.es/prodyser/espa_cifras/2017201728 December 2019
[2] European Biomass Association Statistical reporthttps://bioenergyeurope.org/statistical-report.html201615 December 2019
[3] Ministry of Agriculture and Fisheries Food and environmenthttp://www.mapama.gob.es/es/agricultura/temas/producciones-agricolas/cultivos-herbaceos/arroz/default.aspx201716 January 2020
[4] R Rajamma, R Ball, L Tarelho, G Allen, J A Labrincha, V Ferreira, Characterization and use of biomass fly ash in cement-based materials, J. Hazard Mater. 172 (2–3) (2009) 1049–1060, doi:10.1016/j.jhazmat.2009.07.109.
[5] A Bhardwaj, S K S Hossain, M R Majhi, Preparation and characterization of clay bonded high strength silica refractory by utilizing agriculture wastes, Bol. Soc. Esp. Ceram. Vidr. 56 (2017) 256–262, doi:10.1016/j.bsecv.2017.04.002.
[6] B Chatveera, P Lertwattanaruk, Durability of conventional concretes containing black rice husk ash, J. Environ. Manag. 92 (2011) 59–66, doi:10.1016/j.jenvman.2010.08.007.
[7] A J Prasara, S H Gheewala, Sustainable utilization of rice husk ash from power plants: a review, J. Clean. Prod. 167 (2017) 1020–1028, doi:10.1016/j.jclepro.2016.11.042.
[8] Directive 96/61, Council directive 96/61/EC of 24 september 1996 concerning integrated pollution prevention and control (IPPC), Off. J. L 257 (1996) Ministry of Industry and Energy https://eur-lex.europa.eu/legal-content/EN/ALL/?uri=celex:31996L0061. (Accessed 20 January 2020).
[9] Communication from the Commission to the European Parliament, the Council, the European Economic and Social Committee and the Committee of the Regions, Close the Circle: an EU Action Plan for the Circular Economy, COM/2015/0614 final, 2015.
[10] R I Iacobescu, G N Angelopoulos, P T Jones, B BanPoint, Y Pontikes, Ladle metallurgy stainless steel slag as a raw material in Ordinary Portland Cement production: a possibility for industrial simbiosis, J. Clean. Prod. 112 (2016) 872–881, doi:10.1016/j.jclepro.2015.06.006.
[11] G Liang, H Zhu, Z Zhang, Q Wu, J Du, Investigation of the waterproof property of alkali-activated metakaolin geopolymer added with rice husk ash, J. Clean. Prod. 230 (2019) 603–612, doi:10.1016/j.jclepro.2019.05.111.
[12] M B Ogundiran, H W Nugteren, G J Witkamp, Geopolymerisation of fly ashes with waste aluminium anodising etching solutions, J. Environ. Manag. 181 (2016) 118–123, doi:10.1016/j.jenvman.2016.06.017.
[13] E Papa, V Medri, E Landi, B Ballarin, F Miccio, Production and characterization of geopolymers based on mixed compositions of metakaolin and coal ashes, Mater. Des. 56 (2014) 409–415, doi:10.1016/j.matdes.2013.11.054.

[14] P Duxon, A Fernández-Jiménez, J L Provis, C G Luckey, A Palomo, J S van Deventer, Geopolymer technology: the current state of the art, J. Mater. Sci. 42 (2007) 2917–2933, doi:10.1007/s10853-006-0637-z.
[15] J L Provis, J S J van Deventer, Geopolymers: Structures, Processing, Properties and Industrial Applications, CRC Press, Cambridge UK, 2009.
[16] P Duxson, J L Provis, G C Lukey, J S J van Deventer, The role of inorganic polymer technology in the development of 'green concrete', Cement Concr. Res. 37 (2007) 1590–1597, doi:10.1016/j.cemconres.2007.08.018.
[17] V Živicas, Effect of type and dosage of alkaline activator and temperature on the properties of alkali-activated slag mixtures, Construct. Build. Mater. 21 (7) (2007) 1463–1469, doi:10.1016/j.conbuildmat.2006.07.002.
[18] N C Nasvi, P G Ranjith, J Sanjayan, The permeability of geopolymer at down-hole stress condition: aplication for carbon dioxide sequestration wells, Appl. Energy 102 (2013) 1391–1398, doi:10.1016/j.apenergy.2012.09.004.
[19] J Davidovits, Properties of Geopolymer Cements in Proceedings First International Conference on Alkali Cements and Concretes, 1, SRIBM, 1994 Ukraine.
[20] K Bouguemonh, N Bouzidi, L Mahtout, L Pérez-Villarejo, M L Martínez-Cartas, Effect of acid attack on microstructure ana composition of metakaolin-based geopolymers: the role of alkaline activator, J. Non-Cryst. Solids 463 (2017) 128–137, doi:10.1016/j.jnoncrysol.2017.03.011.
[21] A Narayanan, P Shanmugasundaram, An experimental investigation on fly ash-based geopolymer mortar under different curing regime for thermal analysis, Energy Build. 138 (2017) 539–545, doi:10.1016/j.enbuild.2016.12.079.
[22] R M Novais, L H Buruberri, G Ascensao, M P Seabra, J A Labrincha, Porous biomass fly ash-based geopolymers with tailored thermal conductivity, J. Clean. Prod. 119 (2016) 99–107, doi:10.1016/j.jclepro.2016.01.083.
[23] V Vaou, D Panias, Thermal insulating foamy geopolymers from perlite, Miner. Eng. 23 (2010) 1146–1151, doi:10.1016/j.mineng.2010.07.015.
[24] R M Novais, R C Pullar, J A Labrincha, Geopolymer foams: an overview of recent advancements, Prog. Mater. Sci. 109 (2020) 100621, doi:10.1016/j.pmatsci.2019.100621.
[25] Z N M N Gouloured, B Nait-Ali, S Zekeng, E Kamseu, U C Melo, D Smith, C Leonelli, Recycled natural wastes in metakaolin based porous geopolymers for insulating applications, J. Build Eng. 3 (2015) 58–69, doi:10.1016/j.jobe.2015.06.006.
[26] N N M Zenabou, N Benoit-Ali, S Zekeng, S Rossignol, U C Melo, A B Tchamba, E Kamseu, C Leonelli, Improving insulation in metakaolin based geopolymer: effects of metabauxite and metatalc, J. Build. Eng. 23 (2019) 403–415, doi:10.1016/j.jobe.2019.01.012.
[27] Y Cui, D Wang, J Zhao, D Li, S Ng, Y Rui, Effect of calcium stearate based foam stabilizer on pore characteristics and thermal conductivity of geopolymer foam material, J. Build. Eng. 20 (2018) 21–29, doi:10.1016/j.jobe.2018.06.002.
[28] E Papa, V Medri, D Kpogbemabou, V Morinière, J Laumonier, A Vaccari, Porosity and insulating properties of silica-fume based foams, Energy Build. 131 (2016) 223–232, doi:10.1016/j.enbuild.2016.09.031.
[29] D Ziegler, A Formia, J-M Tulliani, P Palmero, Environmentally-friendly dense and porous geopolymers using fly ash and rice husk ash as raw materials, Materials 9 (2016) E466, doi:10.3390/ma9060466.
[30] H Soltan Hassan, H A Abdel-Gawwad, S R Vásquez García, I Israde-Alcántara, Fabrication and characterization of thermally-insulating coconut ash-based geopolymer foam, Waste Manag. 80 (2018) 235–240, doi:10.1016/j.wasman.2018.09.022.
[31] Z Chen, Y Liu, W Zhu, En-H Yang, Alkali-treated incineration bottom ash as supplementary cementitious materials, Construct. Build. Mater. 112 (2016) 1025–1031, doi:10.1016/j.conbuildmat.2018.05.231.
[32] I Perná, T Hanzlícek, The solidification of aluminum production waste in geopolymer matrix, J. Clean. Prod. 84 (2014) 657–662, doi:10.1016/j.jclepro.2014.04.043.
[33] C Leiva, Y Luna-Galiano, C Arenas, B Alonso-Fariñas, C Fernández-Pereira, A porous geopolimer based on aluminum-waste with acoustic properties, Waste Manag. 95 (2019) 504, doi:10.1016/j.wasman.2019.06.042.
[34] D M A Huiskes, A Keulen, Q L Yu, H J H Brouwers, Design and performance evaluation of ultra-lightweight geopolymer concrete, Mater. Des. 89 (2016) 516–526, doi:10.1016/j.matdes.2015.09.167Get.
[35] R M Novais, L H Buruberri, M P Seabra, D Bajare, J A Labrincha, Novel porous fly ash-containing geopolymers for pH buffering applications, J. Clean. Prod. 124 (2016) 395–404, doi:10.1016/j.jclepro.2016.02.114.
[36] M I M Alzeer, K J D MacKenzie, R A Keyzers, Porous aluminosilicate inorganic polymers (geopolymers): a new class of environmentally benign heterogeneous solid acid, Appl. Catal. Gen. 524 (2016) 173–181, doi:10.1016/j.apcata.2016.06.024.
[37] M Minelli, V Medri, E Papa, F Miccio, E Landi, F Doghieri, Geopolymers as solid adsorbent for CO_2 capture, Chem. Eng. Sci. 148 (2016) 267–274, doi:10.1016/j.ces.2016.04.013.
[38] A A Siyal, M S Muhammad, M Khan, N E Rabat, N Zulfiqar, Z Man, J Siame, K I Azizli, A review on geopolymers as emerging materials for the adsorption of heavy metals and dyes, J. Environ. Manag. 224 (2018) 327–339, doi:10.1016/j.jenvman.2018.07.046.
[39] J Zehua, P Yuansheng, Bibliographic and visualized analysis of geopolymer research and its application in heavy metal immobilization: a review, J. Environ. Manag. 231 (2019) 256–267, doi:10.1016/j.jenvman.2018.10.041.
[40] M Mohammadian, A K Haghi, A study on application of recycled thermosetting plastic, Rev. Rom. Mater. 43 (3) (2013) 276–284.
[41] M A M Al Bakri, H Kamarudin, M Bnhussain, I Khairul Nizar, W I W Mastura, Mechanish and chemical reaction of fly ash geopolymer cement- A review, Asian J. Sci. Res. 1 (5) (2011) 247–253.
[42] A Fernández-Jiménez, A Palomo, M Criado, Microstructure development of alkali activated Fly ash cement: a descriptive model, Cement Concr. Res. 35 (2005) 1204–1209, doi:10.1016/j.cemconres.2004.08.021.
[43] A Fernández-Jiménez, A G de la Torre, A G A Palomo, G López-Olmo, M M Alonso, M A G Aranda, Quantitative determination of phases in the alkaline activation of fly ash. Part II: degree of reaction, Fuel 85 (2006) 1960–1969, doi:10.1016/j.fuel.2006.04.006.
[44] UNE-EN 772-21, Methods of Test for Masonry Units - Part 21: Determination of Water Absorption of Clay and Calcium Silicate Masonry Units by Cold Water Absorption, 2011.
[45] ISO 8301, Thermal Insulation — Determination of Steady-State Thermal Resistance and Related Properties — Heat Flow Meter Apparatus, 1991.
[46] UNE-EN 772-1, Methods of Test for Masonry Units - Part 1: Determination of Compressive Strength, 2011.
[47] M R P Dinakar, H Rao, A review of the influence of source material's oxide composition on the compressive strength of geopolymer concrete, Microporous Mesoporous Mater. 234 (2016) 12–23, doi:10.1016/j.micromeso.2016.07.005.
[48] S S Bhattacharya, G N Chattopadhyay, Increasing bioavailability of phosphorus from fly ash through Vermicomposting, J. Environ. Qual. 31 (2002) 2116–2119, doi:10.2134/jeq2002.2116.
[49] S Ahmari, S X Ren, V Tougfigh, L Zang, Production of geopolymeric binder from blended waste concrete powder and fly ash, Construct. Build. Mater. 35 (2012) 718–729, doi:10.1016/j.conbuildmat.2012.04.044.
[50] V F F Barbosa, K J D MacKenzie, C Thaumaturgo, Synthesis and characterization of materials inorganic polymers of alumina and silica: sodium polysialate polymers, Int. J. Inorg. Mater. 2 (2000) 309–317, doi:10.1016/S1466-6049(00)00041-6.
[51] H Xu, J S J van Deventer, The geopolymerization of alumino-silicate minerals, J. Miner. Proc. 59 (2000) 247, doi:10.1016/S0301-7516(99)00074-5.
[52] A Hajimohammadi, J L Provis, J S J van Deventer, The effect of silica availability on the mechanism of geopolymerisation, Cement Concr. Res. 41 (3) (2011) 210–216, doi:10.1016/j.cemconres.2011.02.001.
[53] M Criado, A Fernández-Jiménez, A Palomo, Alkali activation of fly ash: effect of the SiO_2/Na_2O ratio. Part I: FTIR study, Microporous Mesoporous Mater. 106 (2007) 180–191, doi:10.1016/j.micromeso.2007.02.055.
[54] Z Zang, H Wang, X Yao, Y Zhu, Effects of halloysite in kaolin in the formation an properties of geopolymers, Cement Concr. Compos. 34 (2012) 709–715, doi:10.1016/j.cemconcomp.2012.02.003.
[55] C A Rees, J L Provis, G C Lukey, J S J van Deventer, Attenuated total reflectance Fourier transform infrared analysis of fly ash geopolymer gel aging, Langmuir 23 (2007) 8170–8179, doi:10.1021/la700713g.
[56] K S W Sing, D H Everett, R A W Haul, L Moscou, R A Pierotti, J Rouquerol, Reporting physisorption data for gas/solid systems with special reference to determination of Surface area and porosity, Pure Appl. Chem. 57 (4) (1985) 603–609, doi:10.1515/iupac.57.0007.
[57] N Böke, G D Birch, S M Nyale, L F Petrik, New synthesis method for the production of coal fly ash-based foamed geopolymers, Construct. Build. Mater. 75 (2015) 189–199, doi:10.1016/j.conbuildmat.2014.07.041.
[58] M Thommes, Physical adsorption characterization of nanoporous materials, Chem. Ing. Tech. 82 (2010) 1059–1073, doi:10.1002/cite.201000064.
[59] D Medpelli, J M Seo, D K Seo, Geopolymer with Hierarchically meso/macroporous structures from reactive emulsion templating, J. Am. Ceram. Soc. 97 (2014) 70–73, doi:10.1111/jace.12724.
[60] V Medri, A Ruffini, The influence of process parameters on in situ inorganic foaming of alkali-bonded SiC based foams, Ceram. Int. 38 (2012) 3351–3359, doi:10.1016/j.ceramint.2011.12.045.
[61] E Prud´homme, P Michaud, E Jousseih, C Peyratout, A Smith, S Arrii-Clacens, J M Clacencs, S Rossignol, Silica fume as porogent agent in geo-materials at low temperature, J. Eur. Ceram. Soc. 30 (2010) 1641–1648, doi:10.1016/j.jeurceramsoc.2010.01.014.
[62] E Kamseu, Z N M NGouloure, B Nait Ali, S Zekeng, U C Melo, S Rossignol, C Leonelli, Cumulative pore volume, pore size distribution and phases percolation in porous inorganic polymer composites: relation microstructure and effective thermal conductivity, Energy Build. 88 (2015) 45–56, doi:10.1016/j.enbuild.2014.11.066.
[63] L Dembovska, D Bajare, V Ducman, L Korat, G Bumanis, The use of different by-products in the production of lightweight alkali activated building materials, Construct. Build. Mater. 135 (2017) 315–322, doi:10.1016/j.conbuildmat.2017.01.005.
[64] I Perná, T Hanzlíček, The solidification of aluminum production waste in geopolymer matrix, J. Clean. Prod. 84 (2014) 657–662, doi:10.1016/j.jclepro.2014.04.043.
[65] A Hajimohammadi, T Ngo, P Mendis, J Sanjayan, Regulating the chemical foaming reaction to control the porosity of geopolymer foams, Mater. Des. 120 (2017) 255–265, doi:10.1016/j.matdes.2017.02.026.
[66] D Ziegler, A Formia, J-M Tulliani, P Palmero, Environmentally-friendly dense and porous geopolymers using fly ash and rice husk ash as raw materials, Materials 9 (2016) 466, doi:10.3390/ma9060466.
[67] P Palmero, A Formia, P Antonaci, S Brini, J-M Tulliani, Geopolymer technology for application-oriented dense and lightened materials. Elaboration and characterization, Ceram. Int. 41 (10) (2015) 12967–12979, doi:10.1016/j.ceramint.2015.06.140.
[68] S F Alam Zaidi, E Ul Haq, K Nur, N Ejaz, M Anis-ur-Rehman, M Zubair, M Nave, Synthesis & characterization of natural soil based inorganic polymer foam for thermal insulations, Construct. Build. Mater. 157 (2017) 994–1000, doi:10.1016/j.conbuildmat.2017.09.112.
[69] Z Chen, Y Liu, W Zhu, En-H Yang, Incinerator bottom ash (IBA) aerated geopolymer, Construct. Build. Mater. 112 (2016) 1025–1031, doi:10.1016/j.conbuildmat.2016.02.164.
[70] H Zhang, Building Materials in Civil Engineering, first ed., Woodhead Publishing, 978-1-84569-955-0, 2011.
[71] M Hall, Materials for Energy Efficiency and Thermal Comfort in Buildings, Woodhead Publishing Series in Energy, 978-1-84569-526-2, 2010 Cambridge.

[72] ISO 10456, Building Materials and Products - Hygrothermal Properties – Tabulated Design Values and Procedures for Determining Declared and Design Thermal Values, 2007.
[73] Z N M Ngouloure, B Nait-Ali, S Zekeng, E Kamseu, U C Melo, D Smith, et al., Recycled natural wastes in metakaolin based porous geopolymers for insulating applications, J. Build. Eng. 3 (2015) 58–69, doi:10.1016/j.jobe.2015.06.006.
[74] A Font, M V Borrachero, L Soriano, J Monzó, J Payá, Geopolymer eco-cellular concrete (GECC) based on fluid catalytic cracking catalyst residue (FCC) with addition of recycled aluminium foil powder, J. Clean. Prod. 168 (2017) 1120–1131, doi:10.1016/j.jclepro.2017.09.110.
[75] R M Novais, G Ascensão, N Ferreira, M P Seabra, J A Labrincha, Influence of water and aluminium powder content on the properties of waste-containing geopolymer foams, Ceram. Int. 44 (2018) 6242–6249, doi:10.1016/j.ceramint.2018.01.009.